PHYSICAL REVIEW B VOLUME 28, NUMBER 2 15 JULY 1983

Phonon anomalies in transition-metal nitrides: HfN

A. Nørlund Christensen
Department of Inorganic Chemistry, Aarhus University, DK-8000 Aarhus C, Denmark

W. Kress and M. Miura
Max-Planck-Institut für Festkörperforschung, D-7000 Stuttgart 80, Federal Republic of Germany

N. Lehner
Institut Max von Laue—Paul Langevin, F-38042 Grenoble, France
(Received 8 February 1983)

The phonon dispersion curves in HfN have been measured at room temperature in the high-symmetry directions Δ, Σ, and Λ by coherent inelastic neutron scattering. Anomalies in the dispersion of the acoustic branches have been detected which are similar to those that have already been reported for superconducting transition-metal compounds with nine valence electrons. The experimental results are well described by a double-shell model which is also used to calculate the density of states.

I. INTRODUCTION

Carbides and nitrides of the group-IV*B*, -V*B*, and -VI*B* transition metals form a class of compounds with an unusual and interesting combination of physical properties. They combine covalent characteristics, such as extreme hardness and high melting point, with metallic nature, such as appreciable thermal and electrical conductivity. Almost all these transition-metal carbides and nitrides have the face-centered-cubic rock-salt structure, and for many of them, the phonon dispersion curves have been measured by coherent inelastic neutron scattering.[1–10] The phonon dispersion curves reflect the extreme hardnesses and high melting points by the steep slopes of the acoustic branches in the long-wavelength range and by the relatively high-lying optic branches, separated from the acoustic part of the spectrum by a frequency gap of a few terahertz.

The general nature of the optic branches is, for most of the transition-metal carbides and nitrides, similar to that of ionic compounds with the rock-salt structure. The longitudinal branches (LO) lie above the transverse branches (TO), due to the long-range Coulomb interactions that are screened by the conduction electrons. This metallic screening destroys the Lyddane-Sachs-Teller splitting[11] and results in a degeneracy of the LO and TO modes at the center of the Brillouin zone. However, for most of the transition-metal compounds the screening vector is small compared to the dimensions of the Brillouin zone. The LO branches therefore recover quickly from the screening effect and are for most of the transition-metal carbides and nitrides found above the TO branches. The only exceptions are UC,[3] UN,[5] and, as the results of the present measurements show, HfN.

The most remarkable feature of the transition-metal carbides and nitrides, however, is the appearance of anomalies in the phonon dispersion curves for the compounds that are superconductors. In addition to the correlation between superconductivity and phonon anomalies, a correlation can be established between the number of valence electrons and the occurence of the phonon anomalies. Transition-metal carbides and nitrides with the rock-salt structure and eight valence electrons per unit cell are not superconducting and do not have anomalies in the phonon dispersion curves, but with nine and ten valence electrons the compounds are superconductors and show anomalies. The number of valence electrons can be changed by nonisoelectronic substitution of the metal or nonmetal component or by deviation from stoichiometry (solid solutions and vacancies).

A qualitative understanding of the correlation between the number of valence electrons, the phonon anomalies, and the superconductivity can adequately be obtained from the analysis of the calculated band structures. A rigid band structure is a useful first approximation to the real band structure, and a change in the number of valence electrons will essentially shift the Fermi energy of a rigid electron density of states, from a position in a region of very low density of metal *d* and nonmetal *p* states, upwards into a region of higher density of *p* and *d* states.[12] This leads to a strong electron-phonon coupling that yields the phonon anomalies and the high transition temperatures for superconductivity. This simple qualitative picture is confirmed by the results of first-principles calculations either based on localized wave functions[13] or on a nonorthogonal tight-binding parametrization of the band structure.[14]

The most successful model so far in reproducing the measured phonon dispersion curves of transition-metal carbides and nitrides with rock-salt structure is the double-shell model,[15] which describes the electron-phonon coupling by a second-shell coupling the electrons of the metal sublattice. This additional electronic degree of freedom, which simulates the charge density of the *d* electrons, is treated in the adiabatic approximation. For the analysis of the experimental data, the double-shell model is used.

II. EXPERIMENTAL

A. Crystal preparation

A single crystal of HfN was grown by the zone-annealing technique. A hafnium rod of 99.9% purity

(Koch-Light Laboratories Ltd.) and a diameter of 14 mm was made from four hafnium bars by zone melting in helium of 99.99% purity. The rod was then zone annealed in a nitrogen atmosphere of nominal 99.99% purity at a pressure of 2 MPa and a temperature of approximately 2500 °C for 60 h. In this way the hafnium rod was converted to a single crystal of HfN. Specimens for determination of T_c and the lattice constant were cut from the crystal using spark erosion. The transition temperature for superconductivity was measured to be 8.2 K using an induction method.[16] The lattice constant $a=4.5241(1)$ (Å) was determined from a Guinier powder pattern using Cu$K\alpha$ radiation. The composition $HfN_{0.94(1)}$ was determined gravimetrically by quantitative conversion of hafnium nitride to HfO_2 by ignition in air at 1000 °C for 1 h. The crystallographic direction (110) was nearly parallel to the cylinder axis of the single crystal.

B. Inelastic neutron scattering

A sample with a cylindrical shape and oriented in such a way that the cylinder axis is perpendicular to the scattering plane is considered to be ideal for inelastic neutron scattering measurements on a triple-axis spectrometer. This is only the case, however, if the absorption can be neglected. Inelastic neutron scattering of highly absorbing materials has become feasible with high-flux reactors, and in that case a large cylindrical sample is not well suited for the experiment. In transmission, only small-volume elements located along the two lines in which the bisector of the incoming and the outgoing beam cuts the surface of the cylinder contribute to the scattering. In reflection, only half of the cylindrical surface (to a depth of a few millimeters) contributes to the scattering. In backscattering a maximum of intensity is obtained, and in transmission a minimum is obtained. More intensity can be gained if the cylindrical sample is replaced by a sheetlike sample of the same volume. This sheetlike sample must be oriented perpendicular to the scattering plane with the normal vector of the sample surface parallel (reflection) or perpendicular (transmission) to the bisector of the incoming and outgoing neutron beam.

The cross section for the absorption of thermal neutrons in HfN is 107 b. Based on the considerations outlined above and on precalculations of the planned scans, three approximately 1.8-mm-thick disks with normal vectors (3,3,4.3) were cut by spark erosion from the single crystal. The disks were arranged in a line perpendicular to the (110) scattering plane with aligned normal vectors. The sample obtained in this way had a volume at 1.1 cm^3 and a total mosaic spread of 40′. Measurements were performed in both reflection and transmission. All measurements were carried out at the high-flux reactor of the Institute Laue-Langevin in Grenoble. The phonon dispersion curves in the high-symmetry directions were measured at room temperature. The measurements of the acoustic branches were carried out with the triple-axis spectrometer IN8. The optic branches were studied on the triple-axis spectrometer IN1 which is sited on the hot source. Constant-energy-transfer scans were used for phonons which lay on parts of phonon dispersion curves sufficiently steep to give well-defined peaks. All other phonons were measured with constant-momentum-transfer scans. In Fig. 1 circles and triangles indicate the measured data for longitudinal and transverse phonons, respectively.

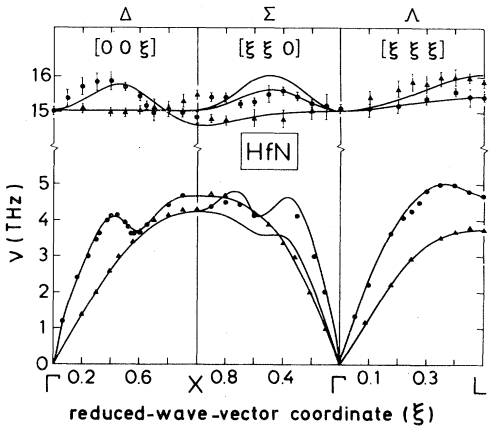

FIG. 1. Phonon dispersion curves for HfN at room temperature. Closed circles and triangles indicate the experimental data for longitudinal and transverse phonons, respectively. The lines represent the results of the double-shell model calculation.

The dispersion curves of HfN are, in many ways, very similar to those of other rock-salt structure transition-metal carbides and nitrides with nine valence electrons per unit cell. At small wave vectors the acoustic branches have steep slopes. Optic and acoustic bands are separated by a frequency gap of about 10 THz. The acoustic branches exhibit the typical anomalies of superconducting transition-metal compounds with nine valence electrons. These anomalies are very pronounced in HfN. The LA branches have minima at $\vec{q}=0.5$ (001), $q=0.55$ (110), and $q=0.5$ (111) (in units of $2\pi/a$).

The above-mentioned features of the phonon dispersion curves of HfN are common to all transition-metal compounds with nine valence electrons that have the rock-salt structure, and were therefore expected. Features which have not been expected were found in the dispersion curves of the optic branches. The most remarkable characteristic of the optical branches in HfN is that the TO branch lies in the whole Λ direction above the LO branch. In the Σ direction, the LO branch has a small minimum at about $\vec{q}=0.7$ (110). In the Δ direction LO and TO branches cross at about $\vec{q}=0.7$ (001). None of these characteristics is found in other transition-metal compounds with nine valence electrons. The only transition-metal compounds that show inverted LO and TO branches in the Λ direction are UC (Ref. 3) and UN (Ref. 5). In UC, the LO and TO branches are nearly degenerate in the whole zone and the small splitting is of the same order of magnitude as the experimental error. UN, however, shows a dispersion of the optical branches very similar to that of HfN. UN has eight valence electrons per unit cell. It is not superconducting and has no anomalies in the dispersion of the acoustic phonons. So far, the measured dispersion of the optic modes in UN has not been reproduced by a theoretical analysis.

TABLE I. Double-shell model parameters for transition-metal carbides and nitrides. Compounds which do not show anomalies are labeled with an asterisk. The force constants are given in units of $e^2/2r_0^3$, the charges Z and Y are given in units of e, and the screening vectors are given in units of π/r_0. $Y_1=0$.

Compound	A_{12}	B_{12}	$A_{22}^{(1)}$	$B_{22}^{(1)}$	$C_{22}^{(1)}$	$A_{11}^{(1)}$	$B_{11}^{(1)}$	Z	Y_2	k_1	k_2	A_2'	B_2'	C_2'	A_2''	B_2''	k'	$k_F=k_s$
TiN[a]	18.53	1.92	11.65	−3.18	0	0	0	−0.70	0	∞	41.6	−0.399	−0.094	−0.043	−0.411	0.021	1.9	0.5
ZrN[b]	15.51	1.12	10.68	−2.71	0	2.29	0.57	−0.62	0	∞	300	−1.108	−0.140	−0.097	−0.696	0.451	5.0	0.3
ZrC*[c]	23.82	3.47	10.02	−1.02	0	0	0	−1.08	−2.0	309	123.5	0	0	0	0	0	∞	0.4
NbN[d]	18.76	1.35	12.64	−2.01	0	0	0	−0.51	0	∞	68.7	1.278	−0.823	−0.622	−0.212	−0.189	10.0	0.2
NbC[c]	19.62	3.96	9.02	−0.70	0	0	0	−0.70	−1.6	726	145.0	−0.713	−0.484	0	−0.943	−0.136	6.0	0.4
TaC[c]	21.65	4.54	10.53	−1.1	0	0	0	−0.71	−1.2	469	145.0	−0.960	−0.640	0	−1.300	−0.120	8.0	0.4
HfC*[c]	22.50	4.60	13.08	−1.77	0	0	0	−1.08	−1.3	180	107.0	0	0	0	0	0	∞	0.4
UC*[e]	11.82	1.20	10.57	−0.44	0	0.21	0	0	0	479	647.0	0	0	0	0	0	∞	0.4
HfN[f]	23.90	−0.16	12.48	1.84	1.91	−0.48	0.12	0	0	∞	106.0	−1.833	−0.539	−0.250	−2.578	0.259	12.5	0
	$A_{22}^{(2)}$	$B_{22}^{(2)}$	$A_{22}^{(3)}$	$B_{22}^{(3)}$														
HfN[g]	−0.711	−0.1223	0.268	2.682														

[a]Reference 7.
[b]Reference 8.
[c]Reference 15.
[d]Reference 10.
[e]$A_{11}^{(2)}=0.42$, $B_{11}^{(2)}=2C_{11}^{(1)}=-0.30$.
[f]This work.

III. THEORETICAL

A. Double-shell model

The measured data were analyzed with a double-shell model.[15] This model has already been used to reproduce the measured phonon dispersion curves of TiN,[7] ZrN,[8] δ-NbN,[10] and the superconducting transition-metal carbides.[2] In the present calculations force constants are taken into account between neighboring nitrogen (subscript 1) and metal (subscript 2) ions (A_{12},B_{12}), between first- $(A_{22}^{(1)},B_{22}^{(1)},C_{22}^{(1)})$, second- $(A_{22}^{(2)},B_{22}^{(2)})$, and third- $(A_{22}^{(3)},B_{22}^{(3)})$ nearest neighbors in the metal sublattice, and between first-nearest neighbors in the nitrogen sublattice $(A_{11}^{(1)},B_{11}^{(1)})$. These forces are assumed to act via inner shells, that carry the charges Y_1 and Y_2. The shells are coupled to their own cores by the force constants k_1 and k_2. The ionic charges are $Z_1=-Z_2$. All Coulomb interactions are screened by the conduction electrons and this screening is taken into account in the Thomas-Fermi approximation. The screening vectors are k_F and $k_s=k_F$. The charge density of the d electrons of the metal sublattice is represented by a second shell around the metal ions. The coupling of this outer shell to the outer shells of first- and second-nearest neighbors in the metal sublattice is described by the force constants A_2',B_2',C_2' and A_2'' and B_2'', respectively. The outer shell is coupled by the force constant k' to the inner shell at the same metal ion site. The outer shells represent an additional electronic degree of freedom which describes the resonancelike softening of the phonon dispersion curves at q vectors, where phonon anomalies occur. The width of the phonon anomalies is a monotonically increasing function of k', whereas the depth of the anomalies is monotonically decreasing with increasing k'. The positions of the anomalies in the Δ and Σ directions depend on the ratio of first- and second-nearest-neighbor coupling constants of the outer shells, A_2' and A_2''. The LA anomaly in the Δ direction occurs at $q=(0,0,0.5)$ when only second-nearest-neighbor couplings between the outer shells are taken into account. When nearest-neighbor couplings become important, the anomaly is shifted towards the zone boundary.

B. Results and discussion

The measured phonon dispersion curves of HfN (Fig. 1) in the Δ direction show only a small LO-TO splitting. The LO-TO splitting at the Γ point in ionic crystals with rock-salt structure is a measure of the strength of the Coulomb interaction. The screening of the conduction electrons reduces this splitting to zero at the Γ point for the transition-metal carbides and nitrides. The dielectric screening function is, however, rapidly decreasing with increasing q and this leads to a maximum splitting between LO and TO in the Δ direction at about $\vec{q}=0.4$ (001) $-\vec{q}=0.6$ (001). This splitting is an indication of the strength of the Coulomb interaction and is very small in HfN. The Coulomb interaction can therefore be neglected and all charges in the model can be put equal to zero. This means that no long-range Coulomb interactions of the cores are taken into account and that the shell displacements lead only to mechanical short-range overlap

TABLE II. Characteristic features of the phonon anomalies in the [00ξ] direction and outer-shell coupling constants for superconducting transition-metal carbides and nitrides.

	Anomalies			Coupling constants			
	Position	Width	Depth				
	(reduced-wave-vector component)		(THz)	k'	A_2'	A_2''	
Compound	ξ	$\Delta\xi$	$\Delta\nu$	$(e^2/2r_0^2)$	$(e^2/2r_0^2)$	$(e^2/2r_0^2)$	$\lvert A_2''/A_2' \rvert$
TiN	0.65	0.3	3.0	1.9	−0.40	−0.41	1.03
ZrN	0.68	0.5	0.5	5.0	−1.11	−0.70	0.63
NbN	1.0	0.6	5	10.0	−1.28	0.21	0.17
NbC	0.65	0.4	1.8	6.0	−0.71	−0.94	1.32
TaC	0.65	0.6	1.2	8	−0.96	−1.30	1.35
HfN	0.58	0.6	1.0	12.5	−1.83	−2.58	1.41

polarization contributions to the dynamical matrix. Furthermore, the polarization of the nitrogen ions can be neglected ($k_1 = \infty$).

The parameters of this model have been determined by a least-squares fit to the measured phonon dispersion curves. The numerical values are listed in Table I. For comparison, the values obtained for the other transition-metal compounds are also reported in Table I. The short-range parameters $A_{12}, B_{12}, A_{22}, B_{22}$ of HfN are in the same range of magnitude as those of the other transition-metal compounds. In Table II the positions and the shapes of the anomalies of various superconducting transition-metal compounds are listed together with the outer-shell parameters. The value of k' is in inversely proportional to the depth of the anomaly. On the other hand, the outer-shell coupling constants are proportional to the width of the anomaly. In HfN the anomaly is very shallow and wide in comparison with TiN. This explains why k' and A_2' and A_2'' are large in HfN. The ratio of A_2'' to A_2' is rather large because the position of the anomaly in the Δ direction of HfN is close to $\vec{q}=(0,0,0.5)$. The large values of A_2' cause a softening of the longitudinal-acoustic branches at and near the zone boundary. To compensate for this softening, which is not observed in the experimental data, interactions to more distant neighbors in the metal sublattices ($A_{22}^{(2)}, A_{22}^{(3)}$) must be taken into account.

According to the large mass ratio and the absence of long-range Coulomb interactions, the optic branches of HfN would be rather flat and nearly degenerate like in UC (Ref. 3) if the first-nearest-neighbor nitrogen-nitrogen interactions ($A_{11}^{(1)}, B_{11}^{(1)}$) are neglected. The coupling constants determined from the measured dispersion curves at room temperature have been used to calculate the one-phonon density of states. The result is shown in Fig. 2. The density of states consists of two narrow bands. The optic band is separated from the acoustic band by an energy gap of about 10 THz.

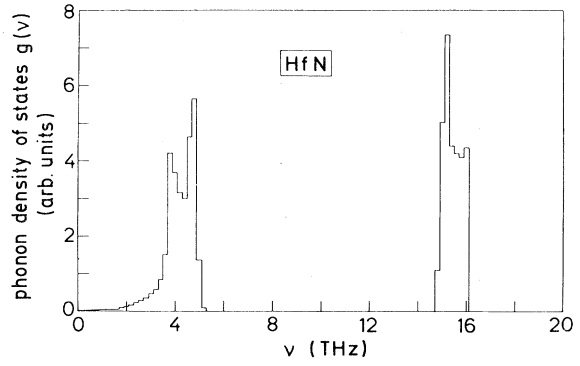

FIG. 2. Calculated one-phonon density of states of HfN.

IV. SUMMARY AND CONCLUSIONS

The measured phonon dispersion curves of HfN show in their acoustic branches the typical features already known from the other superconducting transition-metal carbides and nitrides. The acoustic branches are well described by a double-shell model, and the numerical values for the parameters are similar to those found for other transition-metal compounds.

The optical branches are, however, quite different from those of most other transition-metal compounds. They have only weak dispersion and small splittings of the different branches. This indicates that long-range Coulomb interactions are less important in HfN than in other transition-metal compounds with the exception of UN and UC showing some similarity with HfN. The most interesting feature is the inversion of the LO and TO modes in the Λ direction. In most rock-salt structure compounds the LO modes have higher frequencies than the TO modes, but in HfN, the LO modes are in the whole Λ direction below the TO modes. This means that long-range Coulomb interactions can be neglected and that first-nearest-neighbor nitrogen-nitrogen interactions become important. This interaction indicates a strong overlap of the p-wave functions at neighboring nitrogen atoms.

ACKNOWLEDGMENTS

Two of us (A.N.C. and W.K.) thank the Institut Laue-Langevin for its hospitality. We are grateful to Professor H. Bilz for valuable discussions and constant interest, and one of us (A.N.C.) gratefully acknowledges the Danish Natural Science Research Council and the Carlsbergfondet for financial support.

[1]H. G. Smith and W. Gläser, Phys. Rev. Lett. 25, 1611 (1970).
[2]H. G. Smith and W. Gläser, in *Phonons,* edited by M. A. Nusimovici (Flammarion, Paris, 1971), p. 145.
[3]H. G. Smith, in *Superconductivity in d- and f-Band Transition Metals (Rochester),* Proceedings of the Conference on Superconductivity in *d*- and *f*-Band Metals, edited by D. H. Douglas (AIP, New York, 1972), p. 321.
[4]L. Pintschovius, W. Reichardt, and B. Scheerer, KFK Report No. 2538, 1977 (unpublished), p. 4.
[5]G. Dolling, T. M. Holden, E. C. Svensson, W. J. T. Buyers, and G. H. Lander, in *Lattice Dynamics,* edited by M. Balkanski (Flammarion, Paris, 1978), p. 81.
[6]L. Pintschovius, W. Reichardt, and B. Scheerer, J. Phys. C 11, 1557 (1978).
[7]W. Kress, P. Roedhammer, H. Bilz, W. D. Teuchert and A. N. Christensen, Phys. Rev. B 17, 111 (1978).
[8]A. N. Christensen, O. W. Dietrich, W. Kress, and W. D. Teuchert, Phys. Rev. B 19, 5699 (1979).
[9]W. Weber, P. Roedhammer, L. Pintschovius, W. Reichardt, F. Gompf, and A. N. Christensen, Phys. Rev. Lett. 43, 868 (1979).
[10]A. N. Christensen, O. W. Dietrich, W. Kress, W. D. Teuchert, and R. Currat, Solid State Commun. 31, 795 (1979).
[11]R. H. Lyddane, R. G. Sachs, and E. Teller, Phys. Rev. 59, 673 (1941).
[12]A. Neckel, P. Rastl, R. Eibler, P. Weinberger, and K. Schwarz, J. Phys. C 9, 579 (1976).
[13]W. Hanke, J. Hafner, and H. Bilz, Phys. Rev. Lett. 37, 1560 (1976); W. Hanke, Adv. Phys. 27, 287 (1978).
[14]C. M. Varma and W. Weber, Phys. Rev. Lett. 39, 1094 (1977); Phys. Rev. B 12, 6142 (1979).
[15]W. Weber, Phys. Rev. B 8, 5082 (1973).
[16]A. N. Christensen, S. E. Rasmussen, and G. Thirup, J. Solid State Chem. 34, 45 (1980).